Journal of
Polymer Materials

Tech Science Press

DOI: 10.32604/jpm.2024.056470

ARTICLE

Bio-Nanocomposites Based on Polyvinyl Alcohol and Fuller Earth Nanoclay: Preparation, Properties and Its Application in Food Packaging

Yvonne Achieng Ouma[1], Supriti Sundari Nayak[1], Smrutirekha Mishra[2] and Harekrishna Panigrahi[1,*]

[1]School of Chemical Engineering, Kalinga Institute of Industrial Technology, Deemed to be University Bhubaneswar, Bhubaneswar, Odisha, 751024, India

[2]Department of Materials and Polymer Engineering, Institute of Chemical Technology (ICT) Mumbai-Indian Oil Campus (IOC), Bhubaneswar, Odisha, 751013, India

*Corresponding Author: Harekrishna Panigrahi. Email: harekrishna.panigrahi@kiitbiotech.ac.in; harekrishnapanigrahi91@gmail.com

Received: 23 July 2024 Accepted: 19 September 2024 Published: 16 December 2024

ABSTRACT

Fuller earth (FE) nanoclay is a naturally occurring mineral with a high surface area, is highly abundant, and has a low purchasing cost, making it an excellent candidate for nanocomposite production. The study highlights the novelty of using FE nanoclay in combination with polyvinyl alcohol (PVA) to create a bio-nanocomposite that meets the need for sustainable packaging solutions, underscoring its potential to reduce environmental impact while maintaining product quality in food packaging applications. The solvent casting process, a reliable way to evenly disperse nanofillers in polymer matrices, has been employed in this work to incorporate FE into the polyvinyl alcohol (PVA) matrix to develop PVA/FE bio-nanocomposites. The high-resolution transmission electron microscopy study reveals that the FE nanoclay particles are uniformly dispersed throughout the PVA matrix. The incorporation of 4 wt% of FE into the PVA matrix increases the tensile strength and elongation at break values by 45% and 147%, respectively, which is due to the hydrogen bonding between the hydroxyl groups of PVA and the oxygen atoms present in the FE nanoclay. Incorporation of FE into the PVA matrix has improved the thermal behaviour of the bio-nanocomposites, which is due to the better interfacial interaction between FE and PVA that hinders the early degradation process. The biodegradation study has proved that the bio-nanocomposite film is environmentally friendly, and the coating study results on tomatoes are remarkable, which could be a promising indication of usage in biodegradable packaging and other environmental applications.

KEYWORDS

Polyvinyl alcohol; fullers earth nanoclay; bio-nanocomposites; packaging application

1 Introduction

Polymer nanocomposites have been seen to provide unique mechanical, dynamic mechanical, rheological, and thermal properties often at very low nanofiller weight fractions. Thus, considerable efforts are being directed to evolve newer materials using nanoparticles for the preparation of polymer inorganic hybrids, both with the aim of property enhancement and development of applications [1].

Polymers such as polyamide, polycarbonate, polyolefins, polyvinyl chloride, polystyrene, and others have been widely used for various products from automotive parts and electronics to commodities due to their specific properties suitable for each specific application. They have been filled up with inorganic particles to improve the stiffness and toughness of the materials and enhance their barrier properties [2–4]. Researchers from Toyota discovered the possibility of synthesizing polymer nanocomposites based on nylon-6/organophilic montmorillonite clay that showed dramatic improvements in mechanical and physical properties and heat distortion temperature at very low content of layered silicate [5].

Fuller's earth (FE) is a naturally occurring clay mineral composed mainly of hydrated aluminium silicates. It is abundantly available and composed of kaolinite, montmorillonite, bentonite, and palygorskite [6,7]. It consists of different types of hydrous aluminium silicates with a layered structure that contains ions like Mg^{2+}, Ca^{2+}, K^{+}, NH^{4+}, H^{+}, PO_4^{3-}, SO_4^{2-}, Cl^{-}, NO_3^{3-}, and others [8]. This nanoclay has desirable properties such as high adsorption capacity and low purchasing cost [9]. Its applications include carriers for insecticides, pesticides, and fertilisers used in agriculture and absorbers of oil and water spills on the floors of machine shops, factories, service stations, and other manufacturing plants for safety purposes [10–13].

Polymer and FE nanocomposites have been prepared using different methods such as solution casting, melt mixing, and electrospinning. Bae et al. prepared fully exfoliated nanocomposites by incorporating clay into a polypyrrole graft copolymer [14]. Lim et al. fabricated organic/inorganic hybrid nanocomposites based on poly(styrene–butadiene–styrene) copolymer and clay by melt intercalation [15]. Sancha et al. also synthesized polymer clay nanocomposites using PVA–poly(2-acryl amido-2-methyl-1-propane sulfonic acid) (PAMPS) and FE nanoclay. These nanocomposites show improved thermal and mechanical properties when combined [12].

The consumer demand for biodegradable packaging films is steadily growing as more industries and businesses seek sustainable packaging solutions to reduce the environmental impact caused by the use of non-biodegradable plastics [16]. Many conventional packaging materials provide lack adequate mechanical strength, thermal stability, and barrier properties, leading to food spoilage and reduced shelf life, which is a major concern for consumers and manufacturers. The challenges associated with the use of synthetic materials are proper disposal and biodegradability, which cause serious environmental problems [17–19]. Polyvinyl alcohol (PVA) is a water-soluble synthetic polymer known for its excellent film-forming, adhesive, and biodegradable properties, making it an attractive option for environmentally friendly packaging solutions. Incorporation of FE nanoclay into PVA can significantly enhance the mechanical, thermal, and barrier properties of the resulting nanocomposite material. PVA/FE nanoclay bio-nanocomposite is a promising biodegradable packaging film with several advantages such as improved mechanical properties and thermal stability, making it a viable option for sustainable packaging in food, agriculture, and medicine.

As a result, this research aims to create highly biodegradable polymeric films with enhanced mechanical and thermal properties that can be used in packaging applications whilst being environmentally friendly. In this study, PVA/FE nanocomposite films were prepared using solution casting, a simple and low-cost method. Various characterization methods such as X-ray diffraction (XRD), Fourier transform infrared (FTIR) spectroscopy, thermogravimetric analysis (TGA), high resolution transmission electron microscopy (HRTEM) and universal testing machine have been used to examine the effectiveness and properties of the nanocomposite. The objective of the research on PVA/FE bio-nanocomposite is to improve the characteristics features of PVA films by integrating FE nanoclay to enhance the mechanical strength, thermal stability, biodegradability, and moisture barrier performance, along with the estimation of their all possible applications in sustainable packaging solutions.

2 Experimental

2.1 Materials Used

Polyvinyl alcohol (PVA) (87%–90% hydrolyzed) having an average molecular weight of 30,000–70,000 was purchased from Sigma-Aldrich Chemical Science Company, Saint Louis, MO, USA. FE is sedimentary nanoclay. Commercially available FE nanoclay (hydrated silicate of K, Al, Fe, Na, Mg) was used as a nanofiller.

2.2 Sample Preparation

2.2.1 Preparation of Pristine PVA Film

Pristine PVA was prepared by solution casting method, where 1 g of PVA was dissolved in 30 mL of distilled water at 80°C on a magnetic stirrer at 500 rpm. The solution was left under stirring for 1.5 h and water was added when necessary, till a viscous solution was formed. The viscous solution was then cast on a petri dish and allowed to dry in an oven at 60°C for 12 h until there was no weight change. The average thickness of the film was 0.5 ± 0.05 mm. The composition of the pristine PVA film prepared using the solvent casting method is reported in Table 1.

Table 1: Different sample of PVA/FE bio-nanocomposite films synthesized

Sl. No.	Sample designation	PVA (wt%)	FE nanoclay (wt%)
1	PVA	100	0
2	PVA+1FE	100	1
3	PVA+2FE	100	2
4	PVA+3FE	100	3
5	PVA+4FE	100	4
6	PVA+5FE	100	5
7	PVA+6FE	100	6
8	PVA+7FE	100	7
9	PVA+8FE	100	8

2.2.2 Preparation of PVA/FE Bio-Nanocomposite Films

To prepare PVA/FE bio-nanocomposites film desired amount of FE nanoclay (1, 2, 3, 4, 5, 6, 7 and 8 wt% with respect to the wt% of PVA) was dried in the oven for 2 h at 80°C to remove the moisture and then sonicated for 1 h in 10 mL of distilled water. Simultaneously, 1 g of PVA was dissolved in 30 mL of distilled water at 80°C on a magnetic stirrer at 500 rpm for 30 min. FE nanoclay solution was then added to the PVA solution and left under stirring for 1.5 h adding distilled water when necessary. The viscous solution was then cast on a petri dish and allowed to dry at 60°C for 12 h until there was no weight change. The average thickness of the film was 0.5 ± 0.05 mm. The steps involved in the preparation of PVA/FE bio-nanocomposite samples are shown in Fig. 1. The designation of the PVA/FE bio-nanocomposite samples is represented in Table 1.

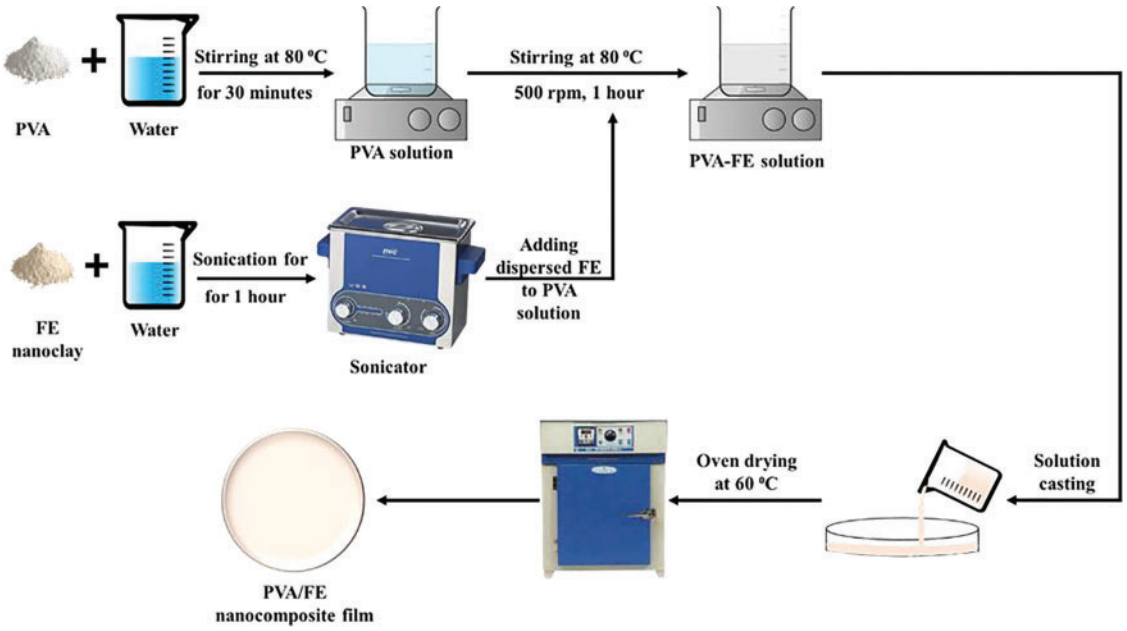

Figure 1: Schematic representation of the preparation of PVA/FE bio-nanocomposite film

2.3 Characterization

2.3.1 Characterization of Pristine FE Nanoclay

Field Emission Scanning Electron Microscopy (FESEM) with Energy Dispersive Analysis of X-Rays (EDAX)

The sonicated FE nanoclay was observed in JSM-7610F plus, JEOL, Tokyo, Japan field emission scanning electron microscope at 5 kV. The elemental composition of the clay was analyzed with the help of JEOL JSM-7610F plus FESEM equipped with Energy Dispersive X-ray analyzer for elemental analysis.

Fourier Transform Infrared Spectroscopy

The characterization functional groups of pristine FE nanoclay were recorded using Fourier transform infrared spectroscopy (FTIR, IRAffinity-1S, Shimadzu, Kyoto, Japan) using the KBr pellet method. The pelleted samples were then scanned over wave number range from 4000 to 500 cm^{-1}. All spectra were reported after an average of 32 scans.

Thermogravimetric Analysis

Thermal stability of FE nanoclay was studied using a thermogravimetric analyzer (TGA, SDT650, TA Instruments, New Castle, DE, USA) in the temperature range of 50°C to 700°C under a high-purity nitrogen flow (at a gas flow rate of 100 mL/min) at a heating rate of 20°C/min.

X-Ray Diffraction

The FE nanoclay was characterized by the X-ray diffraction (XRD) method. For the analysis of the basal spacing of clay, the FE nanoclay powder was mounted on a sample holder with a large cavity, and a smooth surface was obtained by pressing the powder with a glass plate. Powder XRD analysis was performed using a Rigaku MiniFlex diffractometer (Japan) in the range of 10° to 60° using a Cu target ($\lambda = 0.154$ nm) at a scanning rate of 2°/min.

2.4 Characterization of PVA+FE Bio-Nanocomposite Films

2.4.1 Mechanical Properties

Tensile properties of PVA film and PVA+FE bio-nanocomposite films were evaluated with the universal testing machine (UTM) (Model-Z010, Zwick-Roell, Ulm, Germany) at a crosshead speed of 100 mm/min at 25°C with a specimen test length of 40 mm, width of 10 mm, and thickness around 0.5 mm.

2.4.2 Fourier Transform Infrared Spectroscopy

The FTIR spectra analyses of the PVA film and PVA+FE bio-nanocomposite films were recorded using FTIR-ATR spectroscopy (IRAffinity-1S, Shimadzu, Kyoto, Japan) operated at a resolution of 4 cm^{-1}. PVA film and PVA+FE bio-nanocomposite film samples were directly placed on the ray-exposing stage. The spectrum was recorded at a wavenumber of 500–4000 cm^{-1}. All spectra were reported after an average of 32 scans.

2.4.3 Thermogravimetric Analysis

Thermogravimetric analysis of the PVA film and PVA+FE bio-nanocomposite films was carried out using a thermogravimetric analyzer (TGA SDT650, TA Instruments, New Castle, DE, USA) in the temperature range of 50°C to 700°C under a high-purity nitrogen flow (at a gas flow rate of 100 mL/min) at a heating rate of 20°C/min.

2.4.4 High-Resolution Transmission Electron Microscopy (HRTEM)

HRTEM studies of PVA+FE bio-nanocomposite films were performed on thin cryosections of the samples using a JEOL-2100 electron microscope (Tokyo, Japan) with a LaB6 filament. The accelerating voltage was 200 kV. The cryosections of the PVA+FE bio-nanocomposite films were prepared by ultracryomicrotomy by using Leica Ultracut UCT, Leica Microsystems, (Vienna, Austria). Cryosections of 300 nm thickness were achieved by using a Glass knife having a cutting edge of 6°–9°. The sample temperature while performing ultra-cryo-microtomy was kept at −50°C (which was well below the glass transition temperature of the PVA film). The cryosections were cast directly over the copper grids of 300 mesh size.

2.4.5 Biodegradability Study

Small holes were made in a plastic container that was then filled with garden soil. The initial weight of the film samples was weighed and recorded. The samples were completely buried in the soil, and sprinkled with water to keep the soil moist and maintain humidity. The containers were stored at 30°C–35°C. The degradation of the samples was monitored for 3 weeks and weighed at regular intervals of time by removing the samples carefully from the soil and washing them gently with distilled water to remove soil adhering to the surface. They were then dried at 60°C in the oven until constant weight was obtained. The weight loss of the pristine PVA and PVA/FE bio-nanocomposite film was recorded with respect to time.

The biodegradability analysis was calculated by measuring weight loss:

$$\% \text{ weight loss} = \{(\text{Initial weight at the beginning-final weight after 3 weeks})/\text{Initial weight at the beginning}\} * 100$$

2.4.6 Moisture Content Analysis

For moisture content analysis, the pristine PVA and PVA/FE bio-nanocomposite films were first cut into the required sizes. The initial weight of the samples was measured and then the samples were placed inside an oven at 80°C for 12 h. Later, the weight of the films after heat treatment was again measured, and it was ensured that the moisture content of the films was completely eliminated by observing no change in mass with further heating. The moisture content of the films was then determined using the equation:

$$\text{Moisture Content } (\%) = ((W_i - W_f)/W_i) \times 100$$

W_i–Initial weight before drying, W_f–Final weight after drying.

2.4.7 Coating Study of Pristine PVA and PVA/FE Bio-Nanocomposites on Tomatoes

Fresh tomatoes of similar size, shape, color and texture were purchased from the local market. Those were first washed using normal water and then distilled water and dried. The cleaned tomatoes were then dip-coated once with pristine PVA and PVA+4FE bio-nanocomposite solution for ten minutes inside a beaker. Then, the coated tomatoes were taken out from the beaker and the excessive coatings were separated. Then the uncoated and coated tomatoes were placed in petri dish plates in two batches, i.e., at room temperature (~27°C) and inside the refrigerator (~4°C–5°C). The changes were observed and the digital images of each tomato sample were taken between 0 and 21 days using a camera on a daily basis for visual evaluation.

3 Results and Discussion

3.1 Characterization of Pristine FE Nanoclay

The FESEM micrograph of pristine FE nanoclay (Fig. 2a) clearly shows the nano rod-like structure which it possesses. The elemental composition of the pristine FE nanoclay has been analyzed using FESEM equipped with EDX shown in Fig. 2b.

Fig. 2c represents the XRD spectrum for pristine FE nanoclay. A sharp peak for pristine FE nanoclay has been seen at $2\theta = 8.46°$ having an interlayer spacing of 1.064 nm (Fig. 2c).

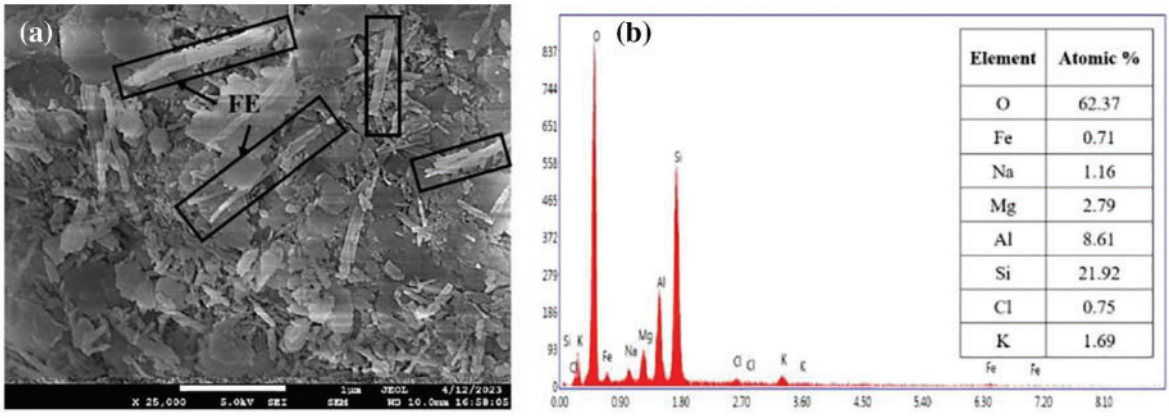

Figure 2: (Continued)

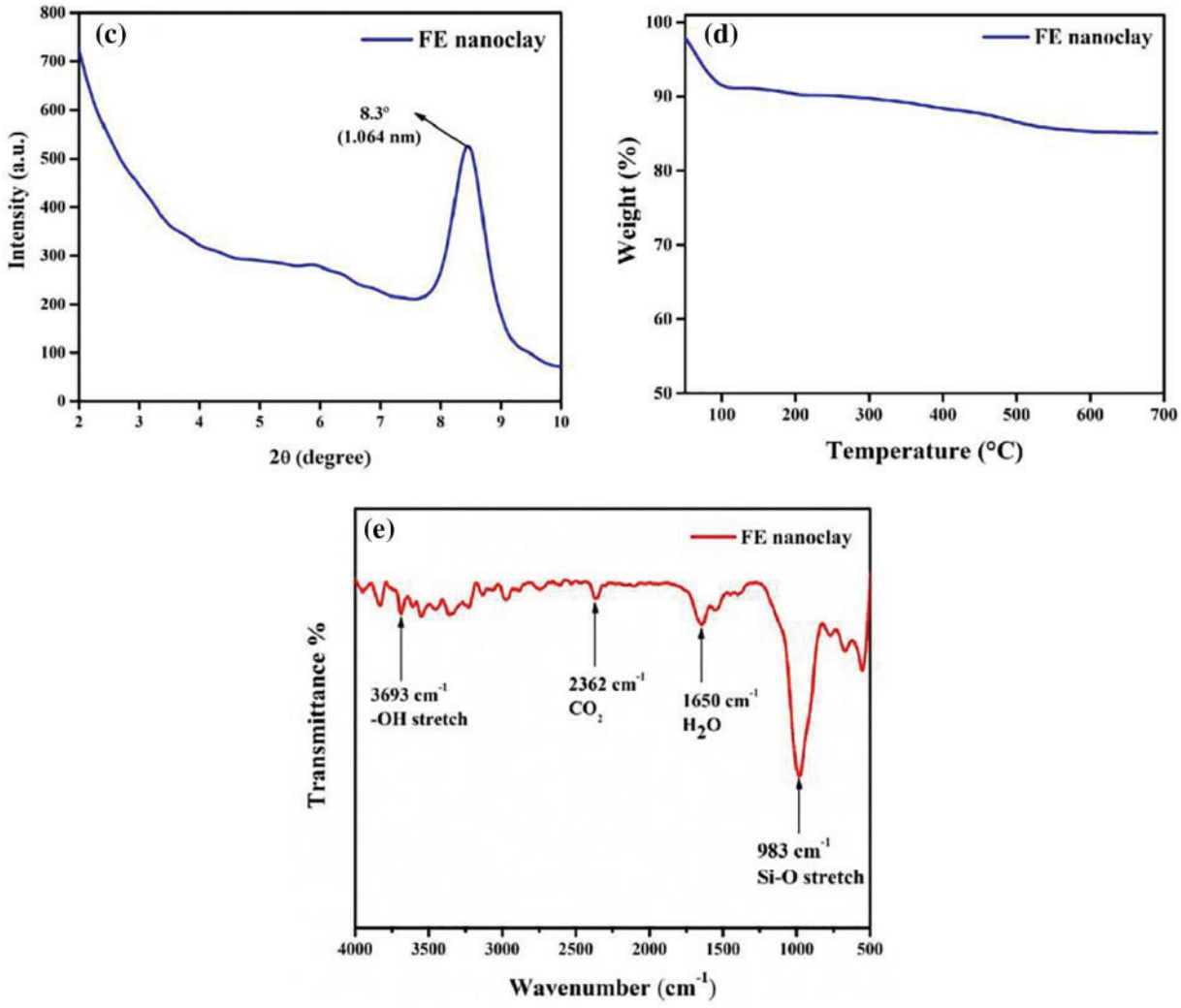

Figure 2: (a) FESEM micrograph of pristine FE nanoclay, (b) Composition of pristine FE nanoclay from FESEM–EDX analysis, (c) XRD spectrum of pristine FE nanoclay, (d) TGA curve of pristine FE nanoclay and (e) FTIR spectrum of pristine FE nanoclay

Fig. 2d represents the TGA curve for pristine FE nanoclay. From the curve, it is clearly observed that the initial weight loss of 8.2%, which is also the major decomposition region of the FE nanoclay; is due to the physisorbed water present in the FE nanoclay. This is due to the physisorbed and interlayer water molecules being mobile and not significantly bound to the surface of the FE nanoclay. This is why these water molecules can be extracted through heat treatment during the process (i.e., below 200°C). The gradual weight loss between 200°C–600°C may be due to the dehydration and dihydroxylation of FE nanoclay [20].

Fig. 2e represents the FTIR spectra for pristine FE nanoclay. In the case of pristine FE, a single sharp peak at 983 cm^{-1} is corresponding to the Si-O vibration (Fig. 2e). The absorption band at 1650 cm^{-1} is attributed to the adsorbed water presence in clay. The corresponding peak at 2362 cm^{-1} present may be due to the atmospheric CO_2 (Fig. 2e). A corresponding peak at 3693 cm^{-1} is assigned to the -OH stretching vibration of the FE nanoclay [21–23].

3.2 Characterization of PVA/FE Bio-Nanocomposites

3.2.1 Mechanical Properties

The tensile-strain study of the PVA/FE bio-nanocomposite films (Fig. 3 and Table 2) has indicated that the tensile strength of PVA nanocomposite increases with the addition of FE nanoclay up to 4 wt% and beyond which it starts to decrease. The PVA+4FE bio-nanocomposite has shown the highest tensile strength among all (Fig. 3). The tensile strength value of PVA+4FE bio-nanocomposite is 45% higher when compared to that of pristine PVA. The increase in tensile strength could be attributed to the improved interfacial bond strength achieved by better dispersion of nanoclay particles in the PVA matrix at lower FE nanoclay loading along with the better interaction of FE nanoclay with PVA and formation of hydrogen bonds. On the contrary, the drop in the tensile strength at greater FE nanoclay loading (Table 2) is likely due to the formation of agglomerates or tactoids, which might have functioned as defects or flaws and crack initiation sites lowering the tensile strength rather than acting as an effective means of dissipating mechanical energy [24–26].

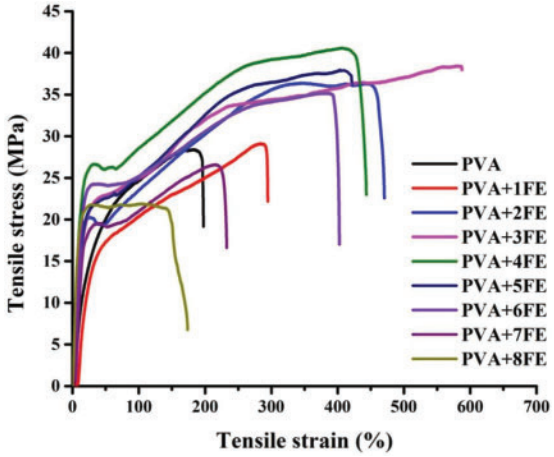

Figure 3: Mechanical properties of pristine PVA and PVA/FE bio-nanocomposites

Table 2: Tensile strength and elongation at break (%) values of pristine PVA and PVA+FE bio-nanocomposites

Sl. No.	Sample	Tensile strength (MPa)	Elongation at break (%)
1.	PVA	28.1 ± 2	180 ± 15
2.	PVA+1FE	29.2 ± 2	295 ± 12
3.	PVA+2FE	36.4 ± 3	470 ± 20
4.	PVA+3FE	38.5 ± 3	585 ± 15
5.	PVA+4FE	40.7 ± 2	445 ± 18
6.	PVA+5FE	37.8 ± 2	420 ± 14
7.	PVA+6FE	35.2 ± 2	400 ± 15
8.	PVA+7FE	26.5 ± 2	235 ± 15
9.	PVA+8FE	21.7 ± 2	175 ± 10

Similarly, elongation at break value is also increased up to 3 wt% of FE nanoclay and then the value gradually decreases up to 8 wt% of FE nanoclay (Fig. 3 and Table 2). The elongation at the break value of PVA+4FE bio-nanocomposite is 225% higher when compared to that of pristine PVA.

Such an increase may be attributed to the least agglomerations and well dispersion of FE nanoclay in the polymer matrix. Therefore, instead of acting as sites of stress concentration, this is making a contribution towards toughening of the polymer matrix. The significant decrease in elongation at break values with increasing FE nanoclay loadings may be due to the rigidity of clay clusters that might have limited the plastic deformation of the polymer matrix [24,25]. Although the elongation of break value is highest in the case of PVA+3FE bio-nanocomposite, overall, the best tensile strength and comparable elongation at break in the case of PVA+4FE bio-nanocomposite is distinguishably high and hence it is the optimum concentration for PVA/FE bio-nanocomposite which is then taken for further investigations.

3.2.2 FTIR Studies

Here for PVA, an absorbance at 3402 cm^{-1} is assigned to the -OH stretching vibrations. The bands observed at 2927 and 2850 cm^{-1} are attributed to CH_2 and C-H asymmetric stretching vibration as shown in Fig. 4. Peaks at 1720 and 1070 cm^{-1} are attributed to the -C=O and C-O stretching vibrations (Fig. 4). In the PVA+4FE bio-nanocomposite (Fig. 4), the peak for Si-O is diminished due to the very low percentage of FE. The curve in the region of 3700–3000 cm^{-1} is also observed in the bio-nanocomposite i.e., for -OH stretching [27–29]. The intermolecular interaction of PVA and FE nanoclay involves a hydrogen bond between hydroxyl groups of PVA and the oxygen atoms present in the clay which is observed with the shifting of -OH stretch in the spectra. There are shifting of other corresponding peaks also observed with respect to PVA due to the interaction of PVA and FE nanoclay and also the spectra of bio-nanocomposite are mostly dominated by PVA. As compared to the spectra of pristine PVA and pristine FE nanoclay, the combined peak of C-O and Si-O stretching in the wavelength of 1077 and 1037 cm^{-1} has shifted in the case of PVA+4FE bio-nanocomposite which supports the formation of polymeric nanocomposite and interaction via hydrogen bonding.

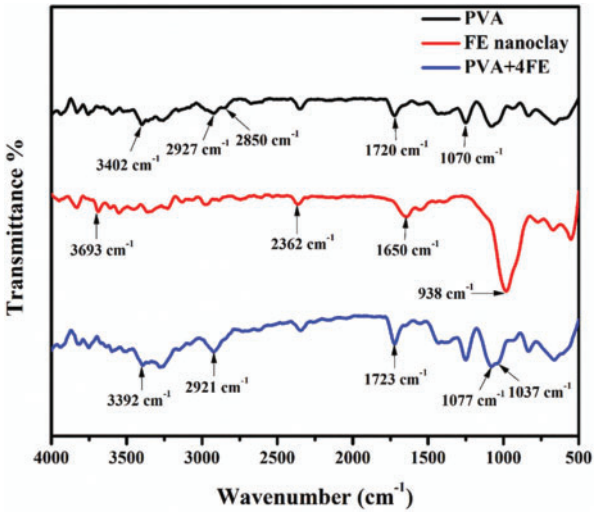

Figure 4: FTIR spectra of pristine PVA, FE nanoclay and PVA+4FE bio-nanocomposite film

3.2.3 Thermogravimetric Analysis (TGA)

TGA and DTG have been carried out to study the effect of FE nanoclay on the thermal stability of PVA (Table 3). From the TGA curve (Fig. 5a) of PVA and PVA+FE bio-nanocomposite, three-phase weight degradation is observed. The first phase degradation before 250°C is due to the evaporation of absorbed free water molecules present in the nanocomposite films. A sharp decrease in the second phase from 250°C–400°C is attributed to the degradation of PVA, i.e., loss of hydroxyl groups as

water, aldehydes and methyl ketones. Above 400°C, third phase decomposition takes place and carbon and hydrocarbons are produced as decomposition products by the degradation of polyene structures [30–32]. The onset degradation temperature (T_i) of PVA+FE bio-nanocomposites shifts to higher temperature with the addition of FE nanoclay up to 4 wt% and beyond that the T_i value decreases. The T_i of PVA+4FE bio-nanocomposite has the maximum value among all (310°C) which is 10°C higher than that of pristine PVA. This improved T_i in the case of PVA+4FE bio-nanocomposite may be due to better dispersion of the nanoclay particles in the PVA matrix hence providing a heat barrier effect. Nevertheless, the decrease in T_i value of PVA+8FE could be due to aggregation of FE nanoclay within the PVA matrix thus less efficient.

Table 3: Effect of FE nanoclay on the thermal stability of PVA

Sl. No.	Sample	Onset of degradation temperature (T_i) (°C)	Maximum degradation temperature (T_{max}) (°C)	Rate of degradation (wt%/min)	% residue at 700°C
1.	PVA	300	319	27.3	0.8
2.	PVA+2FE	303	322	20.7	5.1
3.	PVA+4FE	310	332	20.1	10.5
4.	PVA+8FE	304	335	18.5	11.3

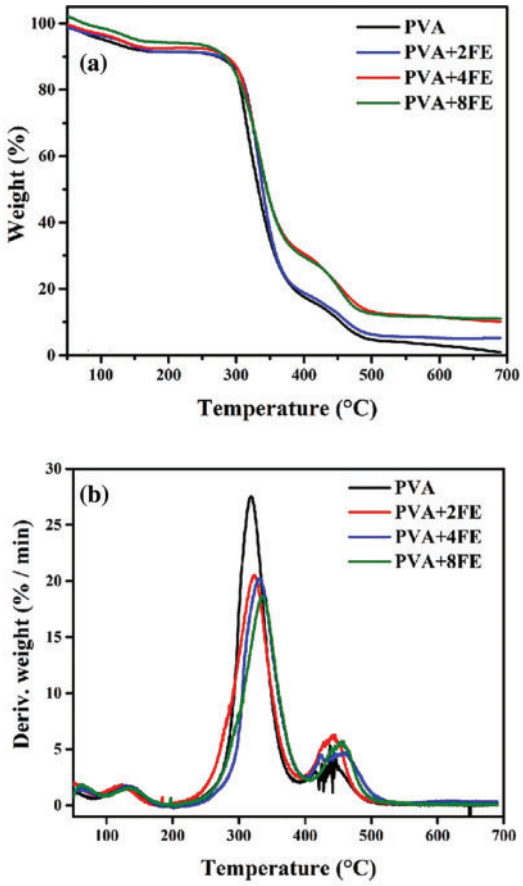

Figure 5: (a) TGA curves of pristine PVA and PVA/FE bio-nanocomposites and (b) DTG curves of pristine PVA and PVA+FE bio-nanocomposites

The rate of degradation of PVA+FE bio-nanocomposites has decreased with the addition of FE nanoclay, i.e., the thermal degradation rate of PVA+FE bio-nanocomposites is comparably lower than that of pristine PVA. This is due to the increased weight % of inorganic FE nanoclay within the nanocomposite. In addition, the higher % residue value trend with the incorporation of FE nanoclay could be due to better interaction of the FE nanoclay with PVA. Insertion of FE nanofiller into the PVA matrix has resulted in improved interfacial interaction between nanofiller and polymer which hinders the degradation process. PVA+8FE results show no remarkable increase compared to that of PVA+4FE. Maximum degradation temperature (T_{max}) increases with the increase of FE nanoclay loading as shown in the curve (Fig. 5b). The T_{max} PVA+FE bio-nanocomposites are comparably higher than that of pristine PVA (Fig. 5b). This may be attributed to the better heat barrier effect of inorganic FE nanoclay within the nanocomposite and thereby improving the heat dissipation for which a continuous increase in T_{max} value has been observed (Table 3).

3.2.4 Morphological Studies Using HRTEM

The distribution of FE nanoclay in the PVA matrix has been studied using HRTEM micrographs of the PVA+FE bio-nanocomposites. The homogeneous dispersion of FE nanoclay particles in the PVA matrix is confirmed by the HRTEM micrograph of the PVA+4FE bio-nanocomposite (Fig. 6a). In the PVA+4FE bio-nanocomposite sample, there is no proof that bulk clay aggregation is present (Fig. 6a). In the end, this improves the physico-mechanical properties of PVA/FE bio-nanocomposites (as mentioned in the earlier sections). The degree of FE nanoclay aggregation increases as the concentration of FE in the PVA matrix rises from 4 to 8 wt% (Fig. 6b), which may be due to the filler-filler interaction. At greater FE nanoclay concentrations (i.e., >4 wt%), this, in turn, decreases the overall physico-mechanical properties of the PVA+FE bio-nanocomposites [33–35].

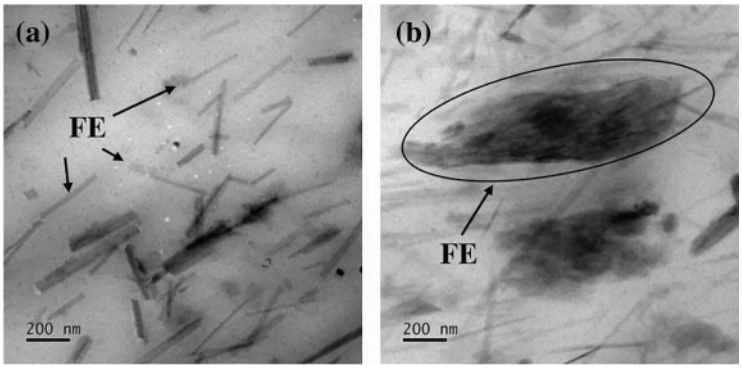

Figure 6: HRTEM micrograph of (a) PVA+4FE and (b) PVA+8FE

3.2.5 Biodegradability Study

The biodegradability study of PVA+FE bio-nanocomposite and pristine PVA has been conducted for 21 days as shown in Table 4 below and % weight loss has been calculated for the whole duration [36]. The degradation studies are important for their application as the environmentally friendly nature and further, these can be accepted as bio-nanocomposites. As shown in the table, weight loss of PVA+FE bio-nanocomposite film and pristine PVA film has been recorded with respect to time. Both the films showed significant % weight loss of more than 3% after 7 days and the weight decreased gradually with an increase in time after 21 days the average % weight loss for PVA+FE bio-nanocomposite film was 36.5% and 26.4% for pristine PVA film. The results obtained revealed that although PVA film is highly degradable, incorporation of FE nanoclay increases the biodegradation rate, making it a suitable nanocomposite for packaging as it will not cause detrimental environmental impact.

Table 4: Biodegradability analysis of PVA and PVA+FE bio-nanocomposites

Sl. No.	Sample	Initial weight (mg)	Weight after 7 days (mg)	Weight after 14 days (mg)	Weight after 21 days (mg)	% weight loss after 21 days
1.	PVA	160.6	155.9	138.5	118.2	26.4
2.	PVA+4FE	155.1	144.9	135.1	98.5	36.5

3.2.6 Moisture Content Analysis

The moisture content analysis of the neat PVA film and PVA+FE bio-nanocomposite films has been performed according to the reported literature [37] and the results are shown in Table 5. It is clear from the table that neat PVA film possesses the highest amount of moisture as compared to the PVA+FE bio-nanocomposites. In the case of PVA+4FE, the lowest value of moisture content is observed and an overall 44.63% less than that of neat PVA. This may be due to the proper dispersion and distribution of FE nanoclay within the PVA matrix which in result creates a barrier that restricts water penetration into the polymeric film [37]. As it can clearly observe from the HRTEM analysis and mechanical study, PVA+4FE has the better dispersion and proper distribution of FE nanoclay within the PVA matrix and above that combination (i.e., from PVA+5FE to PVA+8FE) aggregation of FE nanoclay is observed within the nanocomposite and highest moisture content is observed with the neat PVA film as expected. Also considering the thickness factor of the nanocomposite, the thicker the nanocomposite film, the lesser the moisture content due to the increased diffusion path that the water molecules need to traverse to penetrate the nanocomposite film.

Table 5: Moisture content analysis of PVA and PVA+FE bio-nanocomposites

Sl. No.	Sample	Initial weight (W_i) (in mg)	Final weight (W_f) (in mg)	Moisture content (%)
1.	neat PVA	53.1	48.1	9.41%
2.	PVA+1FE	25.8	23.9	7.36%
3.	PVA+2FE	47.3	43.7	7.61%
4.	PVA+3FE	27.6	25.7	6.88%
5.	PVA+4FE	32.6	30.9	5.21%
6.	PVA+5FE	29.7	27.6	7.07%
7.	PVA+6FE	24.8	23.0	7.25%
8.	PVA+7FE	28.8	26.8	6.94%
9.	PVA+8FE	41.3	39.0	5.56%

3.2.7 Coating Study of Neat PVA and PVA+FE Nanocomposites on Tomatoes

Due to its high nutritional content and health-promoting components, tomatoes are one of the most commercialized fruits. However, plastic packaging materials are employed to reduce perishability since tomatoes have a limited shelf life. Therefore, here we have deployed an alternate packaging option to fulfil the need for eco-friendly packaging in the place of traditional plastics; taking PVA+FE bio-nanocomposites as a coating agent [38–41]. The complete dip-coating experimental process is shown schematically in Fig. 7a. From the taken digital images, it can be clearly observed that the PVA+FE bio-nanocomposite coated tomatoes have maintained better shape, firmness and shelf-life as compared

to neat PVA and without coating. In the case of tomatoes kept at room temperature, no remarkable mold or rottenness was observed at the end of the 9th day in the PVA+FE bio-nanocomposite coated tomatoes when compared to neat PVA coating and without coating (Fig. 7b). At the end of the 18th day, larger mold was observed in the case of non-coated tomatoes indicating complete rottenness whereas in PVA+FE bio-nanocomposite coated tomatoes didn't show any mold or rottenness, only deformation was observed. Similarly, for tomatoes kept inside the refrigerator, there was no mold and deformation till the 12th day and minimal deformation at the end of the 18th day has been observed with the PVA+FE bio-nanocomposite coated tomatoes (Fig. 7c). The shape and the firmness were maintained properly. But tomatoes that were not coated, had shape deformation and ultimately rotted and those coated with neat PVA didn't maintain firmness and shape, and the formation of little bubbles inside the coating was observed. This may be due to the effective barrier properties of PVA+4FE bio-nanocomposite coatings in which FE nanoclay has maximum distribution and proper dispersion inside the nanocomposite which also upholds the inner moisture of tomatoes and thus maintains its natural hydration. The findings demonstrated that these PVA+FE bio-nanocomposite coatings collectively prevent mold formation, contamination, potential spoiling, and moisture loss during storage and can maintain the proper shape and firmness of the tomatoes. Compared to traditional coatings, our PVA+FE bio-nanocomposite coating can preserve tomato quality and extend the duration of storage.

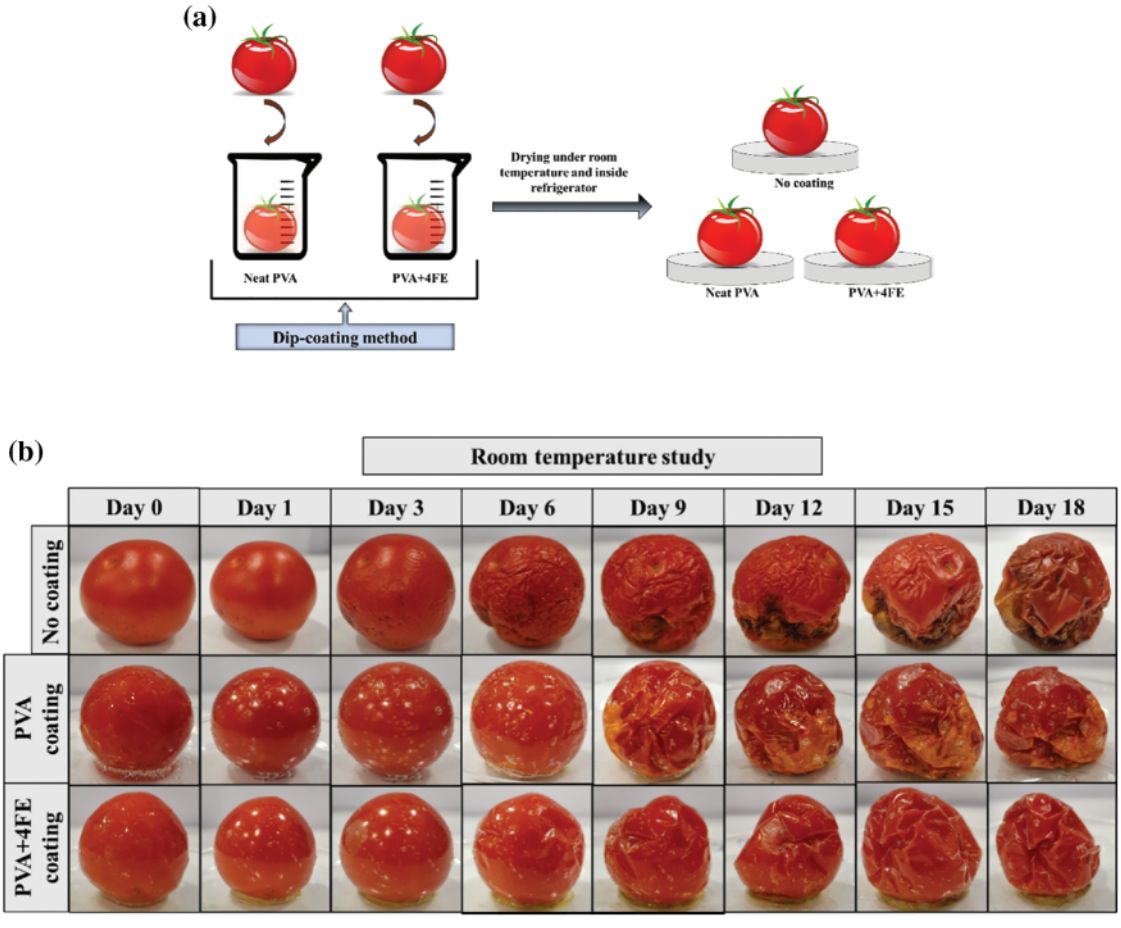

Figure 7: (Continued)

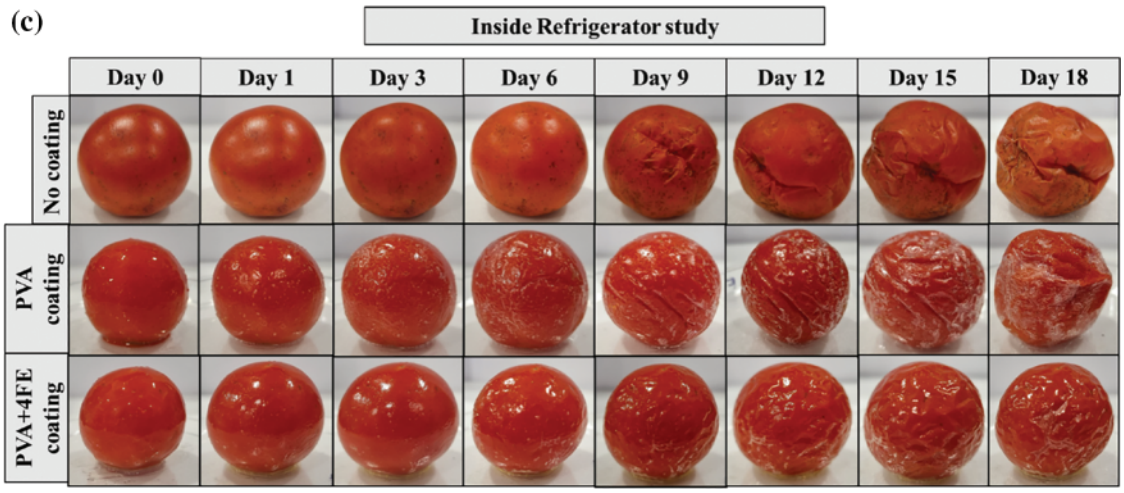

Figure 7: (a) Tomato coating using neat PVA and PVA+FE bio-nanocomposite by dip-coating method is shown schematically. Captured digital images of non-coated and coated tomatoes with neat PVA and PVA+FE bio-nanocomposites at (b) Room temperature, and (c) Inside refrigerator

4 Conclusions

In the present study, PVA is incorporated with FE nanoclay to modify its properties for packaging applications. With regards to mechanical properties, PVA+4FE has shown a significant increase of up to 45% in tensile strength and up to 147% increase in elongation at break compared to that of pristine PVA making it the optimum concentration value for the PVA+FE bio-nanocomposite. The study has also shown that the addition of FE nanoclay can improve the thermal stability of PVA films, making them more resistant to high temperatures. The onset degradation temperature has been revealed to be highest when PVA is loaded with 4 wt% of FE beyond which it decreases due to aggregation of FE nanoclay within the PVA matrix along with a lesser rate of degradation as compared to pristine PVA. PVA+4FE bio-nanocomposite also has the least moisture content among all the nanocomposite combinations and has 44.63% less moisture content than that of neat PVA film. The biodegradability study investigated by soil burial method has also shown that the addition of FE nanoclay increases the biodegradability of the nanocomposite compared to pristine PVA which is found to be 10% more than that of pristine PVA. The most promising application as a coating agent is also validated through the coating of tomatoes with PVA+4FE bio-nanocomposite and better shelf-life, firmness, shape and no rottenness were achieved when compared to uncoated samples. In general, the use of FE nanoclay as a filler in PVA films has the potential to improve the performance and versatility of these polymeric materials in a variety of applications, including packaging, food processing, and biomedical devices. However, further research is needed to fully understand the properties, chemical behavior and potential applications of these promising bio-nanocomposites.

Acknowledgement: The authors thank the Kalinga Institute of Industrial Technology Deemed to be University Bhubaneswar for providing the necessary infrastructure and research facilities.

Funding Statement: This research received no specific grant from any public, commercial, or non-profit funding agencies.

Author Contributions: Yvonne Achieng Ouma: methodology, validation, analysis, data interpretation, writing original draft, visualization. Supriti Sundari Nayak: methodology, validation, data curation, writing review and editing. Smrutirekha Mishra: resources, writing review and editing, supervision.

Harekrishna Panigrahi: conceptualization, resources, writing review and editing, visualization, supervision. All authors reviewed the results and approved the final version of the manuscript.

Availability of Data and Materials: The datasets generated during and/or analysed during the current study are available from the corresponding author upon reasonable request.

Ethics Approval: Not applicable.

Conflicts of Interest: The authors declare no conflicts of interest to report regarding the present study.

References

1. Pandey P, Bhattacharyya AR, Gutch PK, Chauhan RS, Pant SC. Polyvinyl alcohol fuller's earth clay nanocomposite films. J Appl Polym Sci. 2010;115:3005–12. doi:10.1002/app.31399.
2. Rallini M, Kenny JM. Nanofillers in polymers. In: Carlos F, Jasso-Gastinel, José MK, editors. Modification of polymer properties. William Andrew Publishing: Elsevier; 2017. p. 47–86. doi:10.1016/b978-0-323-44353-1.00003-8.
3. Šupová M, Martynková GS, Barabaszová K. Effect of nanofillers dispersion in polymer matrices: a review. Sci Adv Mater. 2021;3:1–25. doi:10.1166/sam.2011.1136.
4. Chan JX, Wong JF, Petrů M, Hassan A, Nirmal U, Othman N, et al. Effect of nanofillers on tribological properties of polymer nanocomposites: a review on recent development. Polymers. 2021;13:2867. doi:10.3390/polym13172867.
5. Cho JW, Paul DR. Nylon 6 nanocomposites by melt compounding. Polymer. 2001;42(3):1083–94. doi:10.1016/s0032-3861(00)00380-3.
6. Murray HH. Traditional and new applications for kaolin, smectite, and palygorskite: a general overview. Appl Clay Sci. 2000;17:207–21. doi:10.1016/s0169-1317(00)00016-8.
7. Hasan S, Iasir ARM, Ghosh TK, Sen Gupta B, Prelas MA. Characterization and adsorption behavior of strontium from aqueous solutions onto chitosan-fuller's earthbeads. Healthcare. 2019;7(52):1–18. doi:10.3390/healthcare7010052.
8. Kulkarni P, Watwe V, Chavan T, Kulkarni S. Artificial neural networking for remediation of methylene blue dye using fuller's earth clay. Current Res Green Sustainable Chem. 2021;4:100131. doi:10.1016/j.crgsc.2021.100131.
9. Khan A, Hassan S, Naqvi J, Kazmi A, Ashraf Z. Surface activation of fuller's earth (bentonite clay) using organic acids. Sci Int. 2015;27:329–32.
10. Harvey CC, Lagaly G. Industrial applications of clay minerals. In: Handbook of clay science. Taupo, New Zealand, Kiel, Germany: Institute of Geological and Nuclear Sciences, Wairakei Research Centre, Institut für Anorganische Chemie, Christian-Albrechts-Universität zu Kiel; 2023.
11. Moraes JDD, Bertolino SRA, Cuffini SL, Ducart DF, Bretzke PE, Leonardi GR. Clay minerals: properties and applications to dermocosmetic products and perspectives of natural raw materials for therapeutic purposes—a review. Int J Pharm. 2017;534:213–9. doi:10.1016/j.ijpharm.2017.10.031.
12. Sancha R, Bajpai J, Bajpai AK. Designing of fullers-earth-containing poly(vinyl.alcohol)-*g*-poly(2-acrylamido-2-methyl-1-propanesulfonic.acid) nanocomposites: swelling and deswellingbehaviors. J Appl Polym Sci. 2010;118:1230–9. doi:10.1002/app.32325.
13. Kulkarni P, Watwe V, Doltade T, Kulkarni S. Fractal kinetics for sorption of methylene blue dye at the interface of alginate fullers earth composite beads. J Mol Liq. 2021;336:116225. doi:10.1016/j.molliq.2021.116225.
14. Bae WJ, Kim KH, Jo WH, Park YH. Exfoliated nanocomposite from polyaniline graft copolymer/clay. Macromolecules. 2004;37:9850–4. doi:10.1021/ma048829b.
15. Lim YT, Park OO. Microstructure and rheological behavior of block copolymer/clay nanocomposites. Korean J Chem Eng. 2001;18:21–5. doi:10.1007/BF02707193.
16. Chen CW, Tang ZP, Ma YR, Qiu WQ, Yang FX, Mei J, et al. Physicochemical, microstructural, antioxidant and antimicrobial properties of active packaging films based on poly(vinyl alcohol)/clay nanocomposite incorporated with tea polyphenols. Prog Org Coat. 2018;123:176–84. doi:10.1016/j.porgcoat.2018.07.001.

17. Bahrami A, Delshadi R, Assadpour E, Jafari S, Williams L. Antimicrobial-loaded nanocarriers for food packaging applications. Adv Colloid Interface Sci. 2020;278:102140. doi:10.1016/j.cis.2020.102140.
18. Sasikala M, Umapathy MJ. Preparation and characterization of pineapple leaf cellulose nanocrystal reinforced gelatin bio-nanocomposite with antibacterial banana leaf extract for application in food packaging. New J Chem. 2018;42:19979–86. doi:10.1039/C8NJ02973C.
19. Chentir I, Kchaou H, Hamdi M, Jridi M, Li S, Doumandji A, et al. Biofunctional gelatin-based films incorporated with food grade phycocyanin extracted from the saharian cyanobacterium *Arthrospira* sp. Food Hydrocoll. 2019;89:715–25. doi:10.1016/j.foodhyd.2018.11.034.
20. Panda AK, Mishra BG, Mishra DK, Singh RK. Effect of sulphuric acid treatment on the physico-chemical characteristics of kaolin clay. Colloids Surf A: Physicochem Eng. 2010;363:98–104. doi:10.1016/j.colsurfa.2010.04.022.
21. Latip W, Knight VF, Khim OK, Mohd Kasim NA, Wan Yunus WMZ, Mohamad Ali MS, et al. Immobilization of mutant phosphotriesterase on fuller's earth enhanced the stability of the enzyme. Catalysts. 2021;11:983. doi:10.3390/catal11080983.
22. Zope I, Dasari A, Yu ZZ. Influence of polymer-clay interfacial interactions on the ignition time of polymer/clay nanocomposites. Materials. 2017;10:935. doi:10.3390/ma10080935.
23. Rezende JCT, Ramos VHS, Oliveira HA, Oliveira RMPB, Jesus E. Removal of Cr(VI) from aqueous solutions using clay from calumbi geological formation, N. Sra. Socorro, SE State, Brazil. In: Materials Science Forum. 2018. vol. 912, p. 1–6. doi:10.4028/www.scientific.net/msf.912.1
24. Prabhu TN, Demappa T. Thermal degradation kinetics, mechanical, and flame retardant properties of epoxy-HDPE fabric-clay composite laminates. J Appl Polym Sci. 2014;131:40751. doi:10.1002/app.40751.
25. Satyanarayana MS, Bhowmick AK, Dinesh Kumar K. Preferentially fixing nanoclays in the phases of incompatible carboxylated nitrile rubber (XNBR)-natural rubber (NR) blend using thermodynamic approach and its effect on physico mechanical properties. Polymer. 2016;99:21–43. doi:10.1016/j.polymer.2016.06.063.
26. Al-Saleh MA, Yussuf AA, Al-Enezi S, Kazemi R, Wahit MU, Al-Shammari T, et al. Polypropylene/-graphene nanocomposites: effects of GNP loading and compatibilizers on the mechanical and thermal properties. Materials. 2019;12:3924. doi:10.3390/ma12233924.
27. Korbag I, Mohamed Saleh S. Studies on the formation of intermolecular interactions and structural characterization of polyvinyl alcohol/lignin film. Int J Environ Stud. 2016;73:226–35. doi:10.1080/00207233.2016.1143700.
28. Mohanapriya MK, Deshmukh K, Chidambaram K, Ahamed MB, Sadasivuni KK, Ponnamma D, et al. Polyvinyl alcohol (PVA)/polystyrene sulfonic acid (PSSA)/carbon black nanocomposite for flexible energy storage device applications. J Mater Sci: Mater Electron. 2017;28:6099–111. doi:10.1007/s10854-016-6287-2.
29. Das M, Sarkar D. Development of room temperature ethanol sensor from polypyrrole (PPy) embedded in polyvinyl alcohol (PVA) matrix. Polym Bull. 2017;75:3109–25. doi:10.1007/s00289-017-2192-y.
30. Devangamath SS, Lobo B, Masti SP. Narasagoudr S. Thermal, mechanical, and AC electrical studies of PVA-PEG–Ag_2S polymer hybrid material. J Mater Sci: Mater Electron. 2020;31:2904–17. doi:10.1007/s10854-019-02835-3.
31. Tsuchiya Y, Sumi K. Thermal decomposition products of poly(vinyl alcohol). J Polym Sci Part A-1: Polym Chem. 1969;7:3151–8. doi:10.1002/pol.1969.150071111.
32. Gilbert J, Kipling J, Mcenaney B, Sherwood J. Carbonization of polymers I—thermogravimetric analysis. Polymer. 1962;3:1–10. doi:10.1016/0032-3861(62)90060-5.
33. Kar DK, Dutta U, Kumar S, Mishra S, Panigrahi H. The overall performance of graphene oxide-reinforced epichlorohydrin rubber nanocomposites. J Rubber Res. 2024;27:61–71. doi:10.1007/s42464-023-00234-2.
34. Kumar KD, Tsou AH, Bhowmick AK. Unique tackification behavior of needle-like sepiolite nanoclay in brominated isobutylene-co-p-methylstyrene (BIMS) rubber. Macromolecules. 2010;43:4184–93. doi:10.1021/ma100472r.
35. Peighambardoust SJ, Zahed-Karkaj S, Peighambardoust SH, Ebrahimi Y, Peressini D. Characterization of carboxymethyl cellulose-based active films incorporating non-modified and Ag or Cu-modified Cloisite 30B and montmorillonite nanoclays. Iran Polym J. 2020;29:1087–97. doi:10.1007/s13726-020-00863-z.
36. Yu Z, Li B, Chu J, Zhang P. Silica *in situ* enhanced PVA/chitosan biodegradable films for food packages. Carbohydr Polym. 2018;184:214–20. doi:10.1016/j.carbpol.2017.12.043.

37. Kalanidhi K, Nagaraaj P. N-doped carbon dots incorporated chitosan/polyvinylpyrrolidone based polymer film for advanced packaging applications. Chem Phys Lett. 2022;805:139960. doi:10.1016/j.cplett.2022.139960.
38. Duguma HT. Potential applications and limitations of edible coatings for maintaining tomato quality and shelf life. Int J Food Sci Technol. 2021;7:1353–66. doi:10.1111/ijfs.15407.
39. Alaş MÖ, Doğan G, Yalcin MS, Ozdemir S, Genç R. Multicolor emitting carbon dot-reinforced PVA composites as edible food packaging films and coatings with antimicrobial and UV-blocking properties. ACS Omega. 2022;7:29967–83. doi:10.1021/acsomega.2c02984.
40. Das TK, Bhawal P, Ganguly S, Mondal S, Remanan S, Ghosh S, et al. Synthesis of hydroxyapatite nanorods and its use as a nanoreinforcement block for ethylene methacrylate copolymer matrix. Polym Bull. 2018;76(7):3621–42. doi:10.1007/s00289-018-2565-x.
41. Das TK, Ganguly S. Revolutionizing food safety with quantum dot-polymer nanocomposites: from monitoring to sensing applications. Foods. 2023;12:2195. doi:10.3390/foods12112195.